frontiers | Frontiers in Remote Sensing

TYPE Original Research
PUBLISHED 16 January 2023
DOI 10.3389/frsen.2022.1085808

Check for updates

OPEN ACCESS

EDITED BY
Steven Michael De Jong,
Utrecht University, Netherlands

REVIEWED BY
Ethan Theuerkauf,
Michigan State University, United States
Ranjeet John,
University of South Dakota, United States

*CORRESPONDENCE
Kelsey Huelsman,
ksh5s@virginia.edu

SPECIALTY SECTION
This article was submitted to Unoccupied Aerial Systems (UASs and UAVs), a section of the journal Frontiers in Remote Sensing

RECEIVED 31 October 2022
ACCEPTED 28 December 2022
PUBLISHED 16 January 2023

CITATION
Huelsman K, Epstein H, Yang X, Mullori L, Červená L and Walker R (2023), Spectral variability in fine-scale drone-based imaging spectroscopy does not impede detection of target invasive plant species. *Front. Remote Sens.* 3:1085808. doi: 10.3389/frsen.2022.1085808

COPYRIGHT
© 2023 Huelsman, Epstein, Yang, Mullori, Červená and Walker. This is an open-access article distributed under the terms of the Creative Commons Attribution License (CC BY). The use, distribution or reproduction in other forums is permitted, provided the original author(s) and the copyright owner(s) are credited and that the original publication in this journal is cited, in accordance with accepted academic practice. No use, distribution or reproduction is permitted which does not comply with these terms.

Spectral variability in fine-scale drone-based imaging spectroscopy does not impede detection of target invasive plant species

Kelsey Huelsman[1]*, Howard Epstein[1], Xi Yang[1], Lydia Mullori[1], Lucie Červená[2] and Roderick Walker[3]

[1]Department of Environmental Science, Unversity of Virginia, Charlottesville, VA, United States, [2]Department of Applied Geoinformatics and Cartography, Charles University, Prague, Czechia, [3]Blue Ridge PRISM, Inc., Charlottesville, VA, United States

Land managers are making concerted efforts to control the spread of invasive plants, a task that demands extensive ecosystem monitoring, for which unoccupied aerial vehicles (UAVs or drones) are becoming increasingly popular. The high spatial resolution of unoccupied aerial vehicles imagery may positively or negatively affect plant species differentiation, as reflectance spectra of pixels may be highly variable when finely resolved. We assessed this impact on detection of invasive plant species *Ailanthus altissima* (tree of heaven) and *Elaeagnus umbellata* (autumn olive) using fine-resolution images collected in northwestern Virginia in June 2020 by a unoccupied aerial vehicles with a Headwall Hyperspec visible and near-infrared hyperspectral imager. Though *E. umbellata* had greater intraspecific variability relative to interspecific variability over more wavelengths than *A. altissima*, the classification accuracy was greater for *E. umbellata* (95%) than for *A. altissima* (66%). This suggests that spectral differences between species of interest and others are not necessarily obscured by intraspecific variability. Therefore, the use of unoccupied aerial vehicles-based spectroscopy for species identification may overcome reflectance variability in fine resolution imagery.

KEYWORDS

hyperspectral, spectral variability, invasive plants, drone, visible, near-infrared, discriminant analysis

1 Introduction

Globally, invasive plants pose significant threats to natural ecosystems (Gurevitch & Padilla, 2004) and biodiversity (Gaertner et al., 2009; Kimothi & Dasari, 2010; Peerbhay et al., 2016). Across the state of Virginia, invasive, non-native plants are radically altering natural environments by inhibiting the growth of native species upon which native wildlife and insects depend (Miller et al., 2013). These widespread changes in species composition also have broader impacts on soil chemistry and forest canopies, with effects on dynamics of carbon, nutrients, water, and energy (Liao et al., 2008; Lovett et al., 2016).

Ailanthus altissima (tree of heaven) is a notably widespread and harmful invasive tree not only in Virginia but across the U.S. (Burkholder, 2010). It tends to impact the soil chemistry and species composition of ecosystems in which it is present by: increasing nutrient cycling rates; increasing soil C, N, K, and Mg; and encouraging the encroachment of other plant species that thrive in high nutrient environments (Gómez-Aparicio & Canham, 2008). *Elaeagnus umbellata*

(autumn olive) is a common invasive shrub; as of 2017, it was found on 39,000 ha in the U.S. (Oliphant et al., 2017). It has a relationship with N-fixing endosymbionts and affects nitrifying (ammonium-oxidizing) microorganisms (Naumann et al., 2010; Malinich et al., 2017), and therefore is especially competitive in disturbed areas with N-poor soils (Malinich et al., 2017). In addition to its tolerance of nutrient-poor conditions, *E. umbellata* is also drought resistant and able to survive in a wide range of soil moisture conditions (Naumann et al., 2010; Malinich et al., 2017). Last, it can outcompete native plants after establishment due to its dense shading (Oliphant et al., 2017).

Land managers are making concerted efforts to control the spread of invasive plant species, a task that demands extensive ecosystem monitoring (Miller et al., 2013). Traditional approaches to ecosystem observation and monitoring are satellite-based and ground-based. Each approach, however, has caveats. Satellite imagery covers large areas but cannot provide fine-scale details, whereas ground surveying, despite its ability to provide fine-scale details, is labor intensive, and is challenging for surveying broad areas. Unoccupied aerial vehicles (UAVs) provide data on an intermediate scale, with much higher spatial resolution than satellite data and with more spatial coverage than ground surveys (Alvarez-Vanhard et al., 2021). As UAVs merge the benefits of more traditional satellite-based and ground-based monitoring, they are becoming an increasingly popular means to observe ecosystems, including invasive plant species monitoring (Sun & Scanlon, 2019).

Whereas UAVs are becoming increasingly popular as a vehicle for invasive plant species monitoring, spectroscopy has been and continues to be used for the remote sensing of plant and ecosystem observation. Spectroscopy, which includes a large number of narrow, contiguous bands, provides detailed spectral information (Kaufmann et al., 2008; Chance et al., 2016), which is influenced by differences in biophysical and biochemical characteristics of plants (Matongera et al., 2016; Yang et al., 2016; Wang et al., 2020), including: pigments (Mahlein et al., 2010; Xiao et al., 2014), such as chlorophyll (Asner & Martin, 2008; Thenkabail et al., 2014; Chance et al., 2016), anthocyanins, and carotenoids (Blackburn, 2007); plant water and vegetation stress (Thenkabail et al., 2014); and leaf N, P, and K (Mutanga et al., 2004; Asner & Martin, 2008; Thenkabail et al., 2014; Chance et al., 2016). Thus, spectroscopic data, which serve as an indication of plant chemical and structural properties, vary within and across ecosystems (Martin & Aber, 1997; Ustin et al., 2004).

Spectra are strongly related to certain biochemical and structural plant traits (Jacquemoud et al., 2009; Ollinger 2010; Kattenborn et al., 2019). Generally, greater spectral variation is associated with species or trait variation (Palmer et al., 2002). Certain wavelengths, such as those associated with upper-canopy pigments, water, and nitrogen, can be analyzed to differentiate among species. Intraspecific (within species) trait variability, however, is sometimes similar to or even greater than interspecific (among species) variation (Jung et al., 2010; Messier et al., 2010; Leps et al., 2011; Auger & Shipley 2013).

Though imaging spectroscopy has been previously used to identify individual plant species (Mishra et al., 2017), particularly invasive species (Chance et al., 2016; Aneece & Epstein, 2017; Kganyago et al., 2017; Skowronek et al., 2017), using spectroscopic sensors in concert with UAVs is a relatively new application for these technologies. Whereas a few UAV-based studies have been successful in identifying individual plant species, this has been accomplished in large monocultures where the target plant is easily distinguished from the surrounding vegetation (Huang & Asner, 2009).

Additionally, UAV imagery has much finer spatial resolution than satellites. It is not known, however, whether the very fine spatial resolution of data provided by UAVs is beneficial or detrimental to the process of differentiation. Smaller pixel size overcomes the challenge of averaged spectral properties of large pixel sizes over heterogeneous landscapes (Underwood et al., 2007). Peña et al. (2013), for example, found that increased resolution from 2.4 m to 1.2 m increased the differentiability of tree species by 25%. Similarly; Roberts et al. (2004) found that plant species were least distinct at the stand scale and most distinct at the branch scale, a scale similar to that of Peña et al. (2013). Detection of invasive plant species is likely improved by the fine spatial resolution that a UAV can achieve, as it does not require large and homogeneous infestation stands. With very fine spatial resolution, however, spectral variation among pixels will be greater than with coarser spatial resolution, which yields a smoothing effect of extreme values. It is expected, then, that spectral variation will be greater with decreasing spatial resolution. It is essential to understand the mechanisms that allow for the detection of target invasive plant species within these fine-resolution images.

To explore the fundamental questions of whether variability caused by fine-resolution spectroscopy enhances or impedes the ability to differentiate plant species, we collected images during the 2020 growing season from forest canopies in northwestern Virginia at the Blandy Experimental Farm (BEF), where invasive species are present and common. We address the following questions:

1) Over which wavelengths do intra-individual and intraspecific variability of target invasive plant species exceed interspecific variability?
2) Can the spectral signal from individual pixels within a tree crown be used to effectively detect target invasive plant species in an image?
3) How much does intra-individual and intraspecific variability of target invasive plant species impede the ability to differentiate among species?

2 Materials and methods

2.1 Study site

Blandy Experimental Farm (BEF), a biological field station owned by the University of Virginia, is located in the Shenandoah Valley in northwestern Virginia (39.06°N, 78.07°W). At 190 m elevation, BEF has a mean annual precipitation of 975 mm, a mean annual temperature of 12°C, and a mean July high temperature of 31.5°C. It contains 80 ha of old fields in various stages of succession (Bowers, 1997).

Aerial spectroscopic data collection took place over three 1-ha fields at BEF, based on their abundance of the invasive plant species of interest, *A. altissima* and *E. umbellata*, along with several other trees, shrubs, forbs, and grasses. The fields are in early-to mid-successional stages and are approximately 20, 25, and 30 years in age (Figure 1; green, blue, and purple polygons, respectively). Each field is located on low-relief topography. The early successional field (green polygon in Figure 1A; Figure 1B) contains abundant invasive shrubs, including *E. umbellata* within a heterogeneous matrix of forbs, graminoids, shrubs, and trees (including *A. altissima*). The 25-year-old early-to-mid-successional field (blue polygon in Figure 1A; Figure 1C) contains

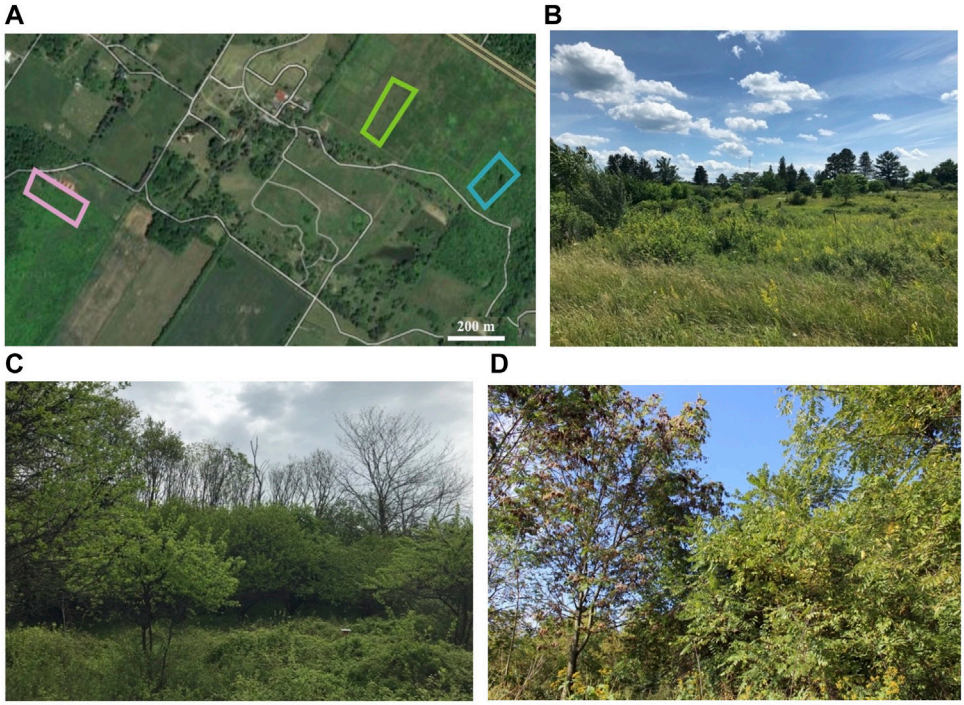

FIGURE 1
(A). Locations of fields in which spectroscopic data were collected during the 2020 growing season. A field in early secondary succession, an intermediate early-to-mid successional field, and a mid-successional field, shown in green, blue, and purple, respectively. **(B)**. Early successional field, which is about 20 years in age and contains abundant invasive shrubs, including *E. umbellata*. **(C)**. Mid-successional field, which is about 30 years in age and contains abundant invasive shrubs, along with *A. altissima*. **(D)**. Early-to-mid successional field, which is about 25 years in age and contains abundant invasive shrubs, including *E. umbellata*.

abundant invasive shrubs, including *E. umbellata*, within a heterogeneous matrix of forbs, graminoids, shrubs, and trees, but with more prevalent trees and shrubs than the early successional field. The mid successional field (purple polygon in Figure 1A; Figure 1D) contains abundant invasive shrubs, along with abundant *A. altissima*.

2.2 Data collection and image post-processing

Spectroscopic images were collected using a DJI Matrice 600 Pro drone equipped with a high-precision GPS system and an imaging spectrometer (Nano-Hyperspec, Headwall Photonics, Bolton, MA). The imaging spectrometer has a spectral range of 400–1,000 nm (in the visible and NIR portions of the electromagnetic spectrum), with a spectral resolution of 2–3 nm over 270 spectral bands. Flight plans over each field were created using universal Ground Control Software (UgCS), in which the UAV would fly in straight lines at a consistent height of 48 m above the ground to obtain images with 3 cm pixels. The imaging spectrometer was programmed to capture images along the flight plan using HyperSpec III software (Headwall Photonics, Bolton, MA).

Images were collected in the middle of the growing season in late June (DOY 178), midday between 10h and 15 h to reduce bidirectional reflectance distribution function (BRDF) effects and under consistent sky conditions. This date of collection was chosen for its proximity to when the National Ecological Observatory Network (NEON) collects spectroscopic images using a fixed-wing aircraft with coarser resolution (approximately 1 m resolution, compared to .03 m resolution). Collected spectroscopic images were adjusted for incoming and scattered solar radiation using a sampled dark reference at the time of flight and a grey scale reference tarp with known reflectance located in the flight scene, respectively. Using HyperSpec III software, terrain and perspective effects were removed with a 1-m digital elevation model provided by the US Geological Survey, and a mosaic of multiple images was created.

2.3 Image sampling

Individuals of 16 tree and shrub species and plant types (*A. altissima*, *Celastrus orbiculatus*, *E. umbellata*, *Gleditsia triacanthos*, *Galium verum*, *Maclura pomifera*, *Juglans nigra*, *Juniperus virginiana*, *Lonicera japonica*, *Lonicera maackii*, *Pinus virginiana*, *Rhamnus davurica*, *Rubus sp.*, *Solidago altissima*, *Symphoricarpos orbiculatus*, and graminoids) were identified in each of the three fields using a high-precision Trimble GPS with measurement accuracy of 0.5 m and used to catalogue individuals within imagery. If a given species was present in images of a field, up to eight individuals were selected for analysis. In cases where fewer than eight individuals were present, as many as were present were sampled.

Within the images, 15 well-lit and representative pixels were selected for spectral sampling from each individual. To remove outliers, a mean was taken across all wavelengths for each reflectance spectrum of a pixel, and a mean was calculated in a similar fashion for all 15 pixels from each individual. Any pixel within an individual that differed more than 25% from the mean

of the individual was removed from the dataset. This removed approximately 1% of pixels from observation.

2.4 Assessing variability due to fine-scale images

Both relative and absolute intraspecific (among individuals within a species) spectral variability were calculated. Relative variability was determined using the coefficient of variation (CV), which compares the variability among the means of each individual to the grand mean of the species. Absolute variability was determined using standard deviation (SD). CV and SD were calculated across all wavelengths for each species. Interspecific (among species) spectral variability was also quantified using CV and SD for comparison to intraspecific variability.

To differentiate *A. altissima* and *E. umbellata*, individuals from Fields E and M were used to train an algorithm with Partial Least Squares Discriminant Analysis (PLS-DA) using the pls R package (Liland et al., 2022). To create an algorithm to detect *A. altissima*, pixels known to be species other than *A. altissima* were recoded into "other" and were separated from *A. altissima*. The same process was followed for *E. umbellata*. Once an algorithm was established using reflectance at each wavelength to separate *A. altissima* and *E. umbellata* pixels in the component space from other species, it was applied to a testing dataset using Field EM, to test the effectiveness of each algorithm. The algorithms to detect *A. altissima* and *E. umbellata* with PLS-DA on the training data were applied to each pixel in the testing dataset. Because the pls R package applies the PLS-DA algorithm to each pixel in both components, only pixels categorized as the species of interest in both components were classified as the species of interest, while pixels categorized as the species of interest in only one component were not.

Then the percentage of pixels within each individual tree or shrub was calculated for each class, and if over half the pixels were classified as the species of interest, the individual was classified as the species of interest. If fewer than half the pixels were classified as the species of interest, the individual was classified as other species. This was done for all individuals using each algorithm to detect both *A. altissima* and *E. umbellata*. Following classification, omission error (false negatives), commission error (false positives), overall accuracy, and Matthew's Correlation Coefficient (MCC; Eq. 1) were calculated. MCC uses the balance of true positives (TP), true negatives (TN), false positives (FP), and false negatives (FN) and can range from −1 to 1, where -1 is entirely incorrect classification and 1 is entirely correct classification. An MCC value of 0 represents classification due to chance.

$$\frac{(TP*TN) - (FP*FN)}{\sqrt{(TP + FP)*(TP + FN)*(TN + FP)*(TN + FN)}} \quad (1)$$

3 Results

3.1 Intra-individual and intraspecific variability relative to interspecific variability

The CV of intra-individual variability exceeded the CV of interspecific variability at 454 nm, 514–663 nm and 694–714 nm in *A. altissima*, with the greatest ratio of relative intra-individual to interspecific variability of 1.42 occurring at 701 nm. The CV of intra-individual variability of *E. umbellata* did not exceed the CV of interspecific variability (Figure 2A). The SD of intra-individual variability exceeded the SD of interspecific variability in *A. altissima* at 530 nm, 570 nm, 574 nm, 583–645 nm, 696–714 nm, and 940 nm and in *E. umbellata* from 450 to 530 nm and 585–705 nm. The greatest ratio of absolute intra-individual to interspecific variability of 1.18 in *A. altissima* occurred at 703 nm and at 459 nm with a ratio of 1.35 in *E. umbellata* (Figure 2B).

The CV of intraspecific variability exceeded interspecific variability in *A. altissima* from 527 to 641 nm and 699–719 nm and in *E. umbellata* from 516 to 521 nm, 603–667 nm, and 690–703 nm. The greatest ratio of relative intraspecific to interspecific variability of 1.29 in *A. altissima* occurred at 703 nm and 1.29 in *E. umbellata* at 696 nm (Figure 3A). The SD of intraspecific variability in *A. altissima* exceeded the SD of interspecific variability at 603 nm, 607 nm, and from 701 to 719 nm and in *E. umbellata* from 450 to 530 nm and 585–705 nm. The greatest ratio of absolute intraspecific to interspecific variability of 1.16 in *A. altissima* occurred at 707 nm and 2.04 in *E. umbellata* at 690 nm (Figure 3B).

3.2 Detection using pixel spectra

The two components of the PLS-DA used to differentiate *A. altissima* pixels from all other species explained a total of 81% of variability in the training data (36% in component 1, and 45% in component 2). *A. altissima* separated most from other species in component 1 and overlapped considerably in the component space (Figure 4A). Wavelengths in the NIR region (763–935 nm) loaded heavily in component 1 (Figure 4B), and wavelengths in the green to yellow spectral region (525–590 nm) loaded heavily in component 2, with the greatest loading values occurring around 540–550 nm (Figure 4C). The two components of the PLS-DA to differentiate *E. umbellata* pixels from all other species explained a total of 72% of variability in the training data (46% in component 1, and 26% in component 2). Unlike *A. altissima*, which separated most in component 1, *E. umbellata* separated from other species in both components and overlapped much less in the component space (Figure 5A). Wavelengths in the blue to green spectral regions (450–510 nm) loaded heavily in component 1 in the negative direction, with a maximum magnitude occurring around 480 nm (Figure 5B). Wavelengths in the red edge region (705–725 nm) loaded most heavily in component 2 (Figure 5C).

Applying the algorithm to the test field to detect *A. altissima* provided an overall accuracy of 66%, with all 3 *A. altissima* individuals (5% of all individuals) falsely classified as not *A. altissima* and 17 individuals (29% of individuals) falsely classified as *A. altissima*. Of the 17 individuals incorrectly classified as *A. altissima*, 5 were *Lonicera maackii*, an invasive shrub, and 3 were *Maclura pomifera* and *Rhamnus davurica*. Overall accuracy to detect *E. umbellata* was 95%, with 7 out of 8 individuals correctly classified as *E. umbellata* and 2 individuals falsely classified as *E. umbellata* (Table 1).

3.3 Variability and differentiation

Wavelengths in the visible spectral region with a ratio of relative intra-individual to interspecific variability (CV) greater than 1 also loaded heavily in component 2 in the PLS-DA to separate *A. altissima* from other species in discriminant analysis (Figure 6A). Wavelengths in the visible and red edge

10.3389/frsen.2022.1085808

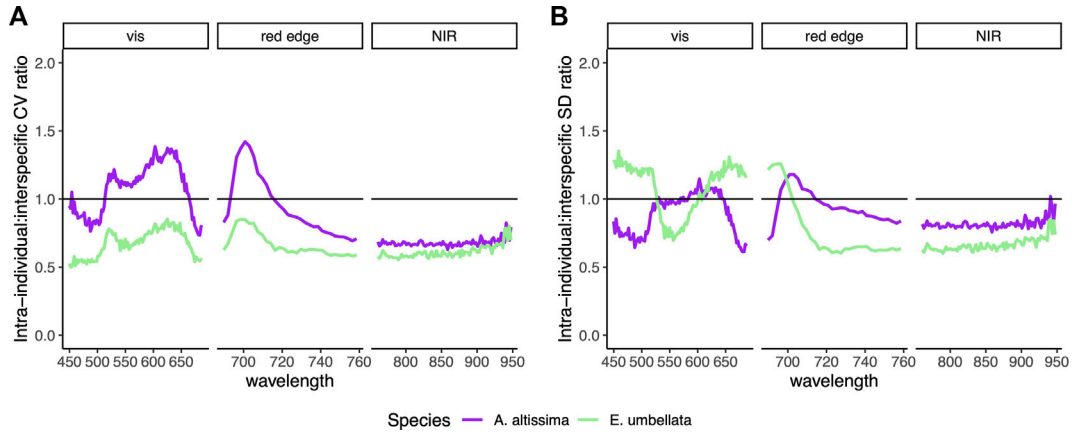

FIGURE 2
(A) Ratio of intra-individual (within individuals, averaged for a single species) to interspecific (among species) coefficient of variation (CV; the variation normalized by mean) across all wavelengths. **(B)** Ratio of intra-individual to interspecific standard deviation (SD) across all wavelengths. Spectra are split into visible, red edge, and near-infrared regions. Ratio values over 1 indicate variability that is greater on average within individuals of a species than among species.

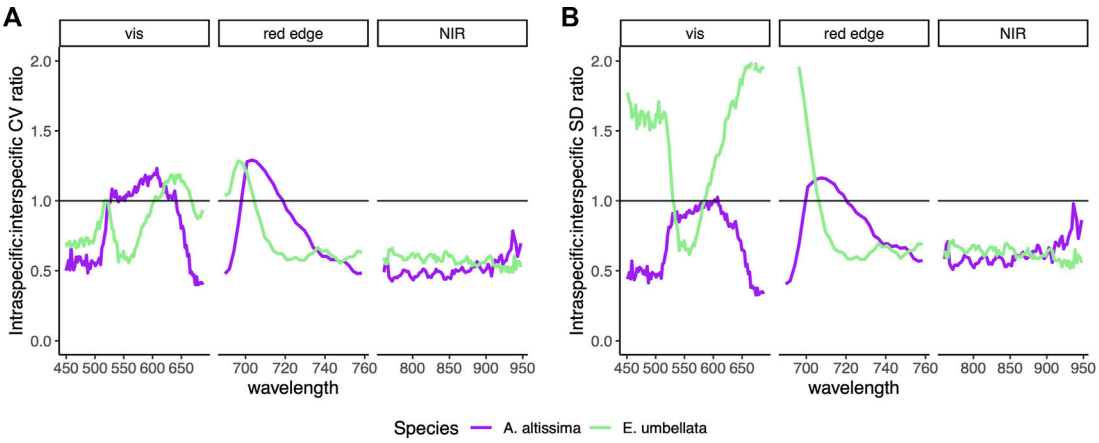

FIGURE 3
(A) Ratio of intraspecific (among individuals within a species) to interspecific (among species) coefficient of variation (CV; the variation normalized by mean) across all wavelengths. **(B)** Ratio of intraspecific to interspecific standard deviation (SD) across all wavelengths. Spectra are split into visible, red edge, and near-infrared regions. Ratio values over 1 indicate variability that is greater on average among individuals within a species than among species.

spectral regions with a ratio of absolute intra-individual to interspecific variability (SD) greater than 1 also loaded heavily in component 1 to separate *E. umbellata* from other species in discriminant analysis (Figure 6B).

Wavelengths in the visible spectral region with a ratio of relative intraspecific to interspecific variability (CV) greater than 1 also loaded heavily in component 2 to separate *A. altissima* from other species in discriminant analysis (Figure 7A). Wavelengths in the visible and red edge spectral regions with ratios of relative and absolute intraspecific to interspecific variability (CV and SD, respectively) greater than 1 also loaded heavily in component 1 to separate *E. umbellata* from other species in discriminant analysis (Figure 7B).

4 Discussion

We utilized both relative (CV) and absolute (SD) variability, as they provide complementary pieces of information; relative variability is calculated by normalizing differences by the mean absolute reflectance values. Normalizing using absolute reflectance values can inflate variability in wavelengths with generally low reflectance values (e.g., visible), compared to those wavelengths with typically higher reflectances (e.g., near infrared). Together however, these two indices provide a more holistic perspective of variability.

Spectral signals from individual pixels detect *E. umbellata* more accurately than *A. altissima*, even with some wavelengths exhibiting absolute intraspecific variability more than twice that of interspecific variability. Despite the overall degree of absolute intraspecific variability for *E. umbellata*, it exceeds interspecific variability over fewer wavelengths compared to *A. altissima*, and the relative variability within *E. umbellata* individuals (intra-individual variability) does not exceed interspecific variability for any wavelength. These patterns suggest that not only degree of variability but also frequency of high levels of variability, metric of variability, and scale at which variability occurs are all of importance.

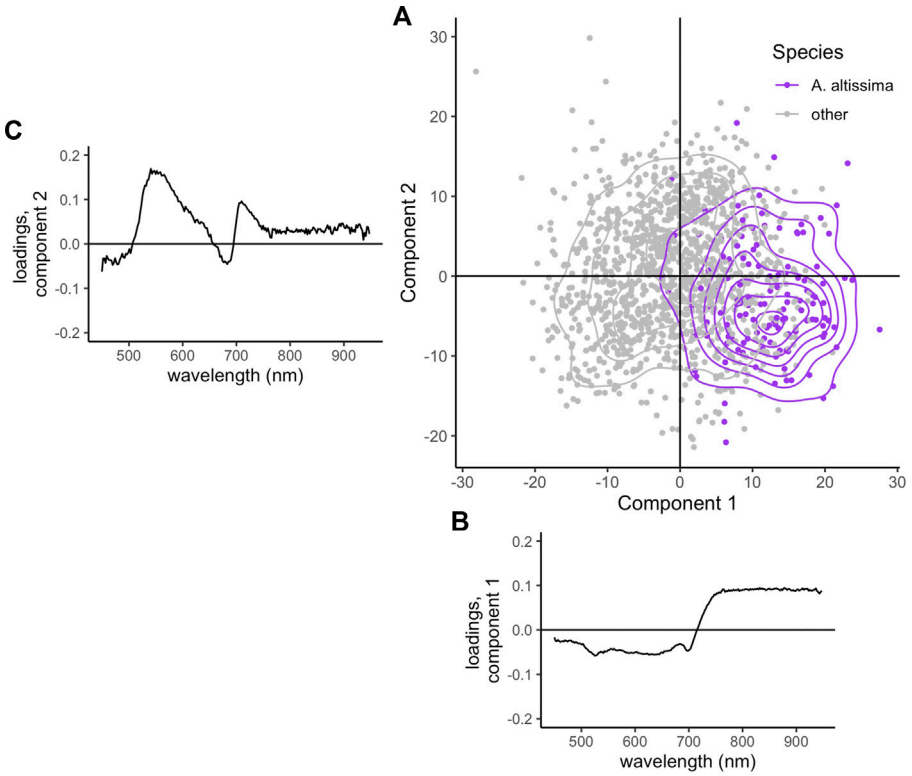

FIGURE 4
(A) Location of all *E. umbellata* training pixels (purple) and all other species (grey) in component space. **(B)** Shown below the *x*-axis is Component 1, and **(C)** beside the *y*-axis are the loadings for each wavelength in Component 2.

Spectral regions in which both relative and absolute intra-individual or intraspecific variability exceed interspecific variability are of interest, as they may hinder differentiation of species. Wavelengths at which both relative and absolute intra-individual variability exceed interspecific variability in *A. altissima* are 530 nm, 570 nm, 574 nm, 583–645 nm, and 696–714 nm. Wavelengths at which both relative and absolute intraspecific variability exceed interspecific variability in *A. altissima* are 603 nm, 607 nm, and 701–719 nm. Wavelengths at which both relative and absolute intraspecific variability exceed interspecific variability in *E. umbellata* are 516–521 nm, 603–667 nm, and 690–703 nm, whereas relative intra-individual variability in *E. umbellata* does not exceed interspecific variability for any wavelengths. Therefore overall variability likely does not impede classification of *E. umbellata* to the same extent as for *A. altissima*.

In addition to considering the degrees to which and frequencies with which intra-individual and intraspecific variability exceed interspecific variability, the specific wavelengths over which variability is high and how they relate to separation in PLS-DA are also important. Intra-individual variability exceeds interspecific variability over some wavelengths that are important for separation in PLS-DA for both species. For *A. altissima*, only relative intra-individual variability exceeds interspecific variability in wavelengths that are important for separation, while absolute intra-individual variability does not. For *E. umbellata*, only absolute intra-individual variability exceeds interspecific variability at wavelengths that are important for separation, while relative intra-individual variability does not. The lack of overlap between wavelengths important for separation and both high relative and absolute variability for each species suggests intra-individual variability likely does not influence classification.

Intraspecific variability also exceeds interspecific variability over some wavelengths that are important for separation in PLS-DA for both species. For *A. altissima*, only relative intraspecific variability exceeds interspecific variability in wavelengths that are important for separation, while absolute intra-individual variability does not. For *E. umbellata*, both absolute and relative intraspecific variability exceed interspecific variability for wavelengths that are important for separation. As both relative and absolute variability are high in wavelengths important for separation of *E. umbellata* from other species, intraspecific variability could potentially influence classification, but intra-individual variability likely does not.

The classification results suggest that differences between the species of interest and all other species are more important than the variability among all species, represented by interspecific variability. The amount of overlap in locations of pixels in the PLS-DA component space further supports that factors in addition to intra-individual and intraspecific variability may affect classification. Not only is classification of *E. umbellata* ultimately more accurate than that of *A. altissima*, but also *A. altissima* overlaps with other species more than *E. umbellata* does in the PLS-DA component space. The lower accuracy of *A. altissima* classification, as well as its location in the PLS-DA component space, suggests that similarities in spectra across

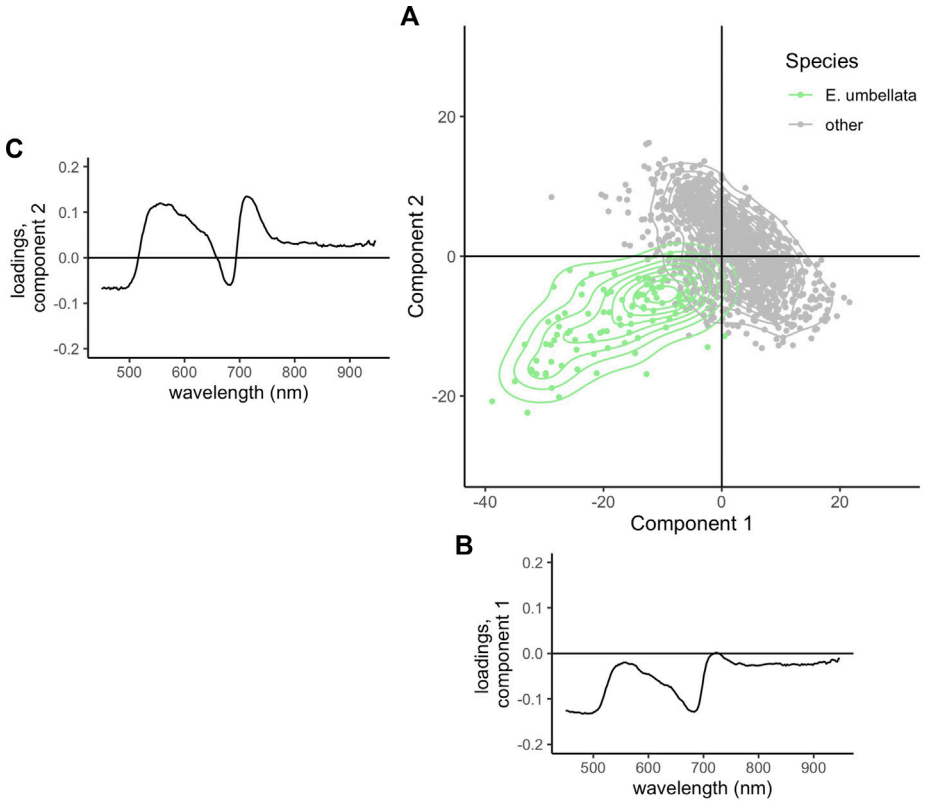

FIGURE 5
(A) Location of all *E. umbellata* training pixels (light green) and all other species (grey) in component space. **(B)** Shown below the *x*-axis is Component 1, and **(C)** beside the *y*-axis are the loadings for each wavelength in Component 2.

TABLE 1 Accuracy of the algorithm to detect A. altissima and E. umbellata in a test field. Individuals were classified based on the classification in each component. True positives and negatives and false positives and negatives are given as number of individuals out of 59 total individuals.

	True positive	True negative	Omission error (false negative)	Commission error (false positive)	Overall accuracy (%)	Matthew's correlation coefficient
A. altissima	0	39	3	17	66	−0.15
E. umbellata	7	49	1	2	95	.96

individuals of multiple species may have a greater impact on detection than intra-individual and intraspecific variability. This implies that *A. altissima* has more spectral features in common with other species, particularly *L. maackii, M. pomifera, and R. davurica*. The similarities of reflectance spectra among a subset of all species are not necessarily captured in the values of interspecific variability, which is why examining pixels in the PLS-DA component space is an additional useful tool.

Traditional hyperspectral data collection efforts are inadequate on the basis of either time or space. For example, satellite data, though temporally robust and therefore providing phenological data, are often too coarse in resolution to detect individual tree and shrub canopies. Collection by fixed-wing aircraft has a finer spatial resolution but is typically collected at much lower frequency, often on an annual basis. Fixed-wing aircraft data collection also requires an open field, which can be a challenge in some forest studies. UAV-based data collection combines the spatial and temporal benefits of each data collection method to provide data with high temporal and spatial resolution. Our results suggest the very fine, leaf-scale resolution of hyperspectral data collected by UAV does not impede differentiation, but rather, the differences among the species of interest and all other species are most important. As these data were collected mid-growing season when phenological differences are least noticeable, utilizing additional dates for differentiation will likely improve detection of invasive plant species.

According to a 2021 literature review (Dainelli et al., 2021), utilizing UAVs to identify invasive plants is not only novel but also tends to be used in concert with RGB, thermal, or multispectral sensors rather than hyperspectral sensors. Researchers who have used hyperspectral imagery to accomplish species recognition and detection have done so in Brazilian tropical forests (Miyoshi et al., 2020a; Miyoshi et al., 2020b), boreal forest (Nezami et al., 2020), and subtropical forest fragments (Sothe et al., 2019) to detect vines, conifers, and broadleaf trees. To our knowledge, this is the first effort to

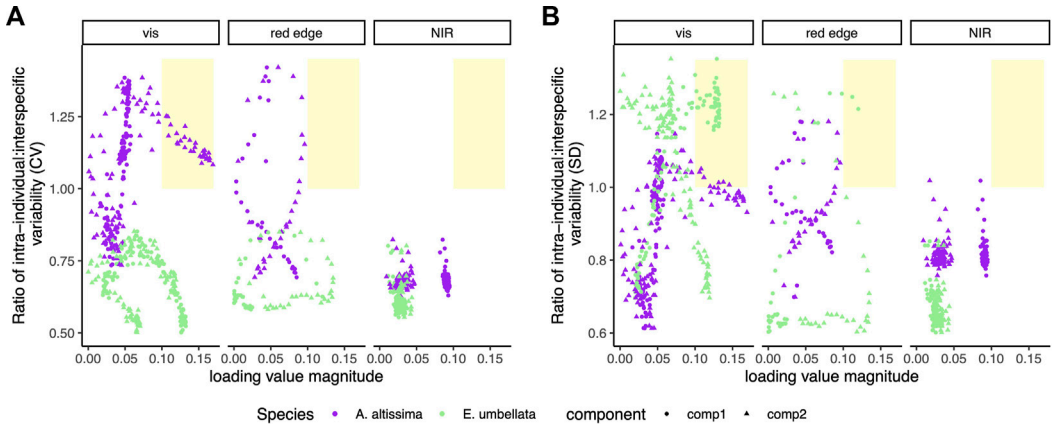

FIGURE 6
Magnitude of loading values for a given wavelength plotted against the ratio of relative and absolute intra-individual to interspecific variability, given as CV **(A)** and SD **(B)**, respectively, for that wavelength. Component 1 and component 2 are shown as circles and triangles, respectively, and *A. altissima* and *E. umbellata* are purple and green, respectively. Wavelengths that both load heavily and have high intra-individual variability relative to interspecific variability are shaded in yellow.

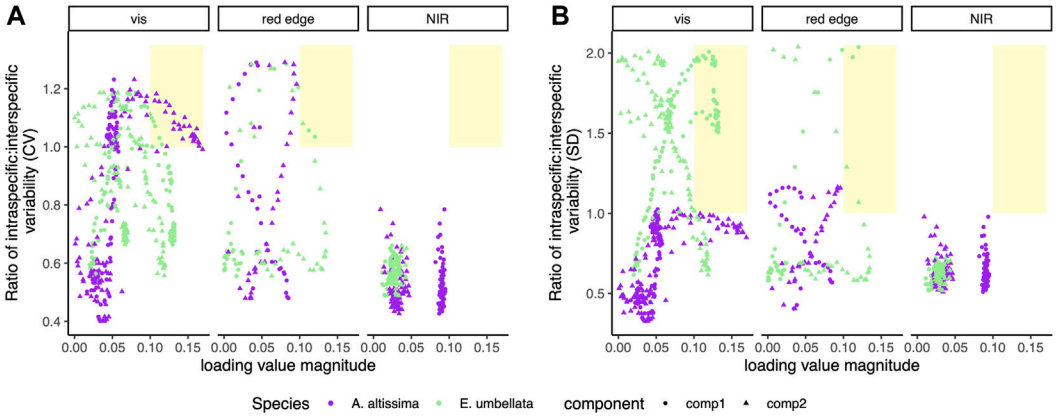

FIGURE 7
Magnitude of loading values for a given wavelength plotted against the ratio of relative and absolute intra-individual to interspecific variability, given as CV **(A)** and SD **(B)**, respectively, for that wavelength. Component 1 and component 2 are shown as circles and triangles, respectively, and *A. altissima* and *E. umbellata* are purple and green, respectively. Wavelengths that both load heavily and have high intra-individual variability relative to interspecific variability are shaded in yellow.

identify and map invasive plant species within heterogeneous vegetation communities using UAV-based hyperspectral data in plant communities typical of the eastern U.S.

We expect to produce an effective general methodology in utilizing spectroscopy to identify and locate targeted invasive plants, although we focused here on the invasive tree *A. altissima* and shrub *E. umbellata* from aerial images. These two invasive plants are commonly occurring across the U.S. and are particularly relevant to the understanding of the ecological impact of invasive species. The conclusion that differences between the species of interest and all other species is more important than intra-individual and intraspecific variability indicates that the temporal flexibility of sampling *via* UAV will aid in the effort of individual species detection. The ability to detect invasive plants allows for the potential to map and monitor their spread. Future work may build on this foundation to generalize detection of these plants in additional plant communities. The addition of spectroscopy in these efforts also provides the opportunity to incorporate an understanding of the variability in plant chemical and structural traits, from canopy to landscape scales.

Data availability statement

The raw data supporting the conclusion of this article will be made available by the authors, without undue reservation.

Author contributions

KH, HE, XY, and RW contributed to conception and design of the study. LČ contributed to field methods. KH and LM organized the

database. KH performed the statistical analysis. KH wrote the first draft of the manuscript. All authors contributed to manuscript revision, read, and approved the submitted version.

Funding

This research was funded by a grant from the USDA (NR 1833A7XXXXG001), the Virginia Space Grant Consortium, and the University of Virginia's Blandy Experimental Farm. LČ was supported by Ministry of Education of the Czech Republic, project LTAUSA18154: Assessment of ecosystem function based on Earth observation of vegetation quantitative parameters retrieved from data with high spatial, spectral and temporal resolution.

Conflict of interest

The authors declare that the research was conducted in the absence of any commercial or financial relationships that could be construed as a potential conflict of interest.

Publisher's note

All claims expressed in this article are solely those of the authors and do not necessarily represent those of their affiliated organizations, or those of the publisher, the editors and the reviewers. Any product that may be evaluated in this article, or claim that may be made by its manufacturer, is not guaranteed or endorsed by the publisher.

References

Alvarez-Vanhard, E., Corpetti, T., and Houet, T. (2021). UAV & satellite synergies for optical remote sensing applications: A literature review. *Sci. Remote Sens.* 3, 100019. doi:10.1016/j.srs.2021.100019

Aneece, I., and Epstein, H. (2017). Identifying invasive plant species using field spectroscopy in the VNIR region in successional systems of north-central Virginia. *Int. J. Remote Sens.* 38, 100–122. doi:10.1080/01431161.2016.1259682

Asner, G. P., and Martin, R. E. (2008). Spectral and chemical analysis of tropical forests: Scaling from leaf to canopy levels. *Remote Sens. Environ.* 112, 3958–3970. doi:10.1016/j.rse.2008.07.003

Auger, S., and Shipley, B. (2013). Inter-specific and intra-specific trait variation along short environmental gradients in an old-growth temperate forest. *J. Veg. Sci.* 24, 419–428. doi:10.1111/j.1654-1103.2012.01473.x

Blackburn, G. A. (2007). Hyperspectral remote sensing of plant pigments. *J. Exp. Bot.* 58, 855–867. doi:10.1093/jxb/erl123

Bowers, M. A. (1997). University of Virginia's blandy experimental farm. *Bull. Ecol. Soc. Am.* 78, 220–225.

Burkholder, A. (2010). Seasonal trends in separability of leaf reflectance spectra for Ailanthus altissima and four other tree species. *Graduate Theses, Diss. Prob. Rep.* 77, 793–804. doi:10.14358/PERS.77.8.793

Chance, C. M., Coops, N. C., Plowright, A. A., Tooke, T. R., Christen, A., and Aven, N. (2016). Invasive shrub apping in an urban nvironment from yperspectral and LiDAR-derived attributes. *Front. Plant Sci.* 7, 1528. doi:10.3389/fpls.2016.01528

Dainelli, R., Toscano, P., Di Gennaro, S. F., and Matese, A. (2021). Recent advances in unmanned aerial vehicles orest emote ensing— systematic eview. Part II: Research pplications. *Forests* 12, 397. doi:10.3390/f12040397

Gaertner, M., Den Breeyen, A., Hui, C., and Richardson, D. (2009). Impacts of alien plant invasions on species richness in mediterranean-type ecosystems: meta-analysis. *Prog. Phys. Geogr.* 33, 319–338. doi:10.1177/0309133309341607

Gómez-Aparicio, L., and Canham, C. (2008). Neighborhood models of the effects of invasive tree species on ecosystem processes. *Ecol. Monogr.* 78, 69–86. doi:10.1890/06-2036.1

Gurevitch, J., and Padilla, D. K. (2004). Are invasive species a major cause of extinctions?. *Trends Ecol. Evol.* 19, 470–474. doi:10.1016/j.tree.2004.07.005

Huang, C.-Y., and Asner, G. P. (2009). Applications of remote sensing to alien invasive plant studies. *Sensors (Basel)* 9, 4869–4889. doi:10.3390/s90604869

Jacquemoud, S., Verhoef, W., Baret, F., Bacour, C., Zarco-Tejada, P. J., Asner, G. P., et al. (2009). PROSPECT+SAIL models: A review of use for vegetation characterization. *Remote Sens. Environ.* 113, S56–S66. doi:10.1016/j.rse.2008.01.026

Jung, V., Violle, C., Mondy, C., Hoffmann, L., and Muller, S. (2010). Intraspecific variability and trait-based community assembly. *J. Ecol.* 98, 1134–1140. doi:10.1111/j.1365-2745.2010.01687.x

Kattenborn, T., Fassnacht, F. E., and Schmidtlein, S. (2019). Differentiating plant functional types using reflectance: hich traits make the difference?. *Remote Sens. Ecol. Conservation* 5, 5–19. doi:10.1002/rse2.86

Kaufmann, H., Segl, K., Guanter, L., Hofer, S., Förster, K.-P., Stuffler, T., et al. (2008). "Environmental apping and nalysis program (EnMAP)–recent advances and status," in IGARSS 2008–2008 IEEE International Geoscience and Remote Sensing Symposium, Boston, MA, USA, 07–11 July, 2008.

Kganyago, M., Odindi, J., Adjorlolo, C., and Mhangara, P. (2017). Selecting a subset of spectral bands for mapping invasive alien plants: Case of discriminating parthenium hysterophorus using field spectroscopy data. *Int. J. Remote Sens.* 38, 5608–5625. doi:10.1080/01431161.2017.1343510

Kimothi, M. M., and Dasari, A. (2010). Methodology to map the spread of an invasive plant (*Lantana camara* L.) in forest ecosystems using Indian remote sensing satellite data. *Int. J. Remote Sens.* 31, 3273–3289. doi:10.1080/01431160903121126

Leps, J., Bello, F., Šmilauer, P., and Doležal, J. (2011). Community trait response to environment: Disentangling species turnover vs intraspecific trait variability effects. *Ecography* 34, 856–863. doi:10.1111/j.1600-0587.2010.06904.x

Liao, C., Peng, R., Luo, Y., Zhou, X., Wu, X., Fang, C., et al. (2008). Altered ecosystem carbon and nitrogen cycles by plant invasion: Meta-analysis. *New Phytol.* 177, 706–714. doi:10.1111/j.1469-8137.2007.02290.x

Liland, K. H., Mevik, B.-H., Wehrens, R., and Hiemstra, P. (2022). pls: Partial least squares and principal component regression. Available at: https://CRAN.R-project.org/package=pls (Accessed October 14, 2022).

Lovett, G., Weiss, M., Liebhold, A., Holmes, T., Leung, B., Lambert, K., et al. (2016). Nonnative forest insects and pathogens in the United States: Impacts and policy options. *Ecol. Appl.* 26, 1437–1455. doi:10.1890/15-1176

Mahlein, A.-K., Steiner, U., Dehne, H.-W., and Oerke, E.-C. (2010). Spectral signatures of sugar beet leaves for the detection and differentiation of diseases. *Precis. Agric.* 11, 413–431. doi:10.1007/s11119-010-9180-7

Malinich, E., Lynn-Bell, N., and Kourtev, P. S. (2017). The effect of the invasive Elaeagnus umbellata on soil microbial communities depends on proximity of soils to plants. *Ecosphere* 8, e01827. doi:10.1002/ecs2.1827

Martin, M. E., and Aber, J. D. (1997). High pectral resolution emote ensing of orest anopy lignin, itrogen, and cosystem rocesses. *Ecol. Appl.* 7, 431–443. doi:10.1890/1051-0761(1997)007

Matongera, T., Mutanga, O., and Lottering, R. (2016). Detection and mapping of bracken fern weeds using multispectral remotely sensed data: A review of progress and challenges. *Geocarto Int.* 33, 209–224. doi:10.1080/10106049.2016.1240719

Messier, J., McGill, B. J., and Lechowicz, M. J. (2010). How do traits vary across ecological scales? A case for trait-based ecology. *Ecol. Lett.* 13, 838–848. doi:10.1111/j.1461-0248.2010.01476.x

Miller, J. H., Manning, S. T., and Enloe, S. F. (2013). *A management guide for invasive plants in southern forests*. Asheville, NC: U.S. Department of Agriculture Forest Service, Southern Research Station.

Mishra, P., asaari, M., shahrimie, M., Herrero-Langreo, A., Lohumi, S., Diezma, B., et al. (2017). Close range hyperspectral imaging of plants: A review. *Biosyst. Eng.* 164, 49–67. doi:10.1016/j.biosystemseng.2017.09.009

Miyoshi, G., Imai, N. N., Garcia Tommaselli, A. M., Antunes de Moraes, M. V., and Honkavaara, E. (2020a). Evaluation of yperspectral multitemporal information to improve ree pecies identification in the highly diverse atlantic orest. Available at: https://10.3390/rs12020244 (Remote sensingAccessed November 21, 2022).

Miyoshi, G. T., Arruda, M., dos, S., Osco, L. P., Marcato Junior, J., Gonçalves, D. N., et al. (2020b). A novel deep earning ethod to identify single ree pecies in UAV-ased yperspectral images. *Remote Sens.* 12, 1294. doi:10.3390/rs12081294

Mutanga, O., Skidmore, A. K., and Prins, H. H. T. (2004). Predicting *in situ* pasture quality in the Kruger national Park, South Africa, using continuum removed absorption features. *Remote Sens. Environ.* 89, 393–408. doi:10.1016/j.rse.2003.11.001

Naumann, J. C., Bissett, S. N., Young, D. R., Edwards, J., and Anderson, J. E. (2010). Diurnal patterns of photosynthesis, chlorophyll fluorescence, and PRI to evaluate water stress in the invasive species, Elaeagnus umbellata Thunb. *Elaeagnus umbellata Thunb. Trees* 24, 237–245. doi:10.1007/s00468-009-0394-0

Nezami, S., Khoramshahi, E., Nevalainen, O., Pölönen, I., and Honkavaara, E. (2020). Tree pecies lassification of drone yperspectral and RGB magery with deep earning convolutional neural networks. *Remote Sens.* 12, 1070. doi:10.3390/rs12071070

Oliphant, A. J., Wynne, R. H., Zipper, C. E., Ford, W. M., Donovan, P. F., and Li, J. (2017). Autumn olive (*Elaeagnus umbellata*) presence and proliferation on former surface coal mines in Eastern USA. *Biol. Invasions* 19, 179–195. doi:10.1007/s10530-016-1271-6

Ollinger, S. V. (2011). Sources of variability in canopy reflectance and the convergent properties of plants. *New Phytol.* 189, 375–394. doi:10.1111/j.1469-8137.2010.03536.x

Palmer, M. W., Earls, P. G., Hoagland, B. W., White, P. S., and Wohlgemuth, T. (2002). Quantitative tools for perfecting species lists. *Environmetrics* 13, 121–137. doi:10.1002/env.516

Peerbhay, K., Mutanga, O., Lottering, R., Bangamwabo, V., and Ismail, R. (2016). Detecting bugweed (*Solanum mauritianum*) abundance in plantation forestry using multisource remote sensing. *ISPRS J. Photogramm. Remote Sens. C* 121, 167–176. doi:10.1016/j.isprsjprs.2016.09.014

Peña, M. A., Cruz, P., and Roig, M. (2013). The effect of spectral and spatial degradation of hyperspectral imagery for the Sclerophyll tree species classification. *Int. J. Remote Sens.* 34, 7113–7130. doi:10.1080/01431161.2013.817712

Roberts, D., Ustin, S., Ogunjemiyo, S., Greenberg, J., Dobrowski, S., Chen, J., et al. (2004). Spectral and structural measures of northwest orest egetation at eaf to landscape cales. *Ecosystems* 7, 545–562. doi:10.1007/s10021-004-0144-5

Skowronek, S., Ewald, M., Isermann, M., Van De Kerchove, R., Lenoir, J., Aerts, R., et al. (2017). Mapping an invasive bryophyte species using hyperspectral remote sensing data. *Biol. Invasions* 19, 239–254. doi:10.1007/s10530-016-1276-1

Sothe, C., Dalponte, M., Almeida, C. M., Schimalski, M. B., Lima, C. L., Liesenberg, V., et al. (2019). Tree pecies lassification in a highly diverse subtropical orest integrating UAV-ased photogrammetric point cloud and yperspectral ata. *Remote Sens.* 11, 1338. doi:10.3390/rs11111338

Sun, A. Y., and Scanlon, B. R. (2019). How can big ata and machine learning benefit environment and water management: Survey of methods, applications, and future directions. *Environ. Res. Lett.* 14, 073001. doi:10.1088/1748-9326/ab1b7d

Thenkabail, P. S., Gumma, M. K., Teluguntla, P., and Mohammed, I. A. (2014). Hyperspectral emote ensing of egetation and agricultural crops. *Photogramm. Eng. Remote Sens. (PE&RS)* 80, 697–723.

Underwood, E., Ustin, S., and Ramirez, C. (2007). A comparison of patial and pectral image resolution for apping nvasive lants in coastal California. *Environ.* 39, 63–83. doi:10.1007/s00267-005-0228-9

Ustin, S. L., Roberts, D. A., Gamon, J. A., Asner, G. P., and Green, R. O. (2004). Using maging pectroscopy to study cosystem rocesses and roperties. *BioScience* 54, 523–534. doi:10.1641/0006-3568(2004)054[0523:UISTSE]2.0.CO;2

Wang, Z., Chlus, A., Geygan, R., Ye, Z., Zheng, T., Singh, A., et al. (2020). Foliar functional traits from imaging spectroscopy across biomes in eastern North America. *New Phytol.* 228, 494–511. doi:10.1111/nph.16711

Xiao, Y., Zhao, W., Zhou, D., and Gong, H. (2014). Sensitivity nalysis of egetation eflectance to biochemical and biophysical variables at eaf, anopy, and regional cales. *IEEE Trans.* 52, 4014–4024. doi:10.1109/TGRS.2013.2278838

Yang, X., Tang, J., Mustard, J. F., Wu, J., Zhao, K., Serbin, S., et al. (2016). Seasonal variability of multiple leaf traits captured by leaf spectroscopy at two temperate deciduous forests. *Remote Sens. Environ.* 179, 1–12. doi:10.1016/j.rse.2016.03.026